

THERMAL ABSORPTION IN SEEDED GASES

MAY 1966

By
Valerie C. Burkig

Distribution of this report is provided in the
interest of information exchange. Responsibility
for the contents resides with the author
or organization that prepared it.

Prepared under Contract No. NASw-1310
by Douglas Aircraft Company, Inc.
Missile and Space Systems Division
Santa Monica, California
for
NATIONAL AERONAUTICS AND SPACE ADMINISTRATION

THERMAL ABSORPTION IN SEEDED GASES

by Valerie C. Burkig

SUMMARY

This report covers the work accomplished during the first 6 months of the contract.

Measurements have been made of the maximum temperature rise achieved when dispersions of fine particles of graphite, iron, tungsten, tantalum carbide, and tungsten carbide in helium have been exposed to the radiation from a xenon flash tube with a black-body temperature of 8,000°K.

Independent measurements of the amount of radiant energy incident on the seeded gas and of the room temperature absorptivity of the dispersions have been used to calculate the expected temperature rise, if energy losses are ignored. For most conditions of gas pressure and seed density used, this temperature has been found to significantly exceed the observed temperature rise.

It has been calculated that reradiation will not limit the rise for temperatures lower than 5,000°K. Nevertheless, measured temperatures greater than 3,300°K have not yet been achieved.

A program is outlined for the second half of the contract period to determine the nature of the processes responsible for limiting the temperature rise. The work will also be extended to hydrogen gas.

INTRODUCTION

In current concepts of the gaseous core reactor, the propellant flow bypasses the fissioning gas region. Energy transfer is by thermal radiation in a wavelength region where hydrogen is normally transparent. The resulting plasma becomes opaque to thermal radiation only at temperatures in excess of $5,000^{\circ}\text{K}$, where hydrogen is dissociated and partly ionized. It has been suggested that fine particles of refractory materials be dispersed in the gas to provide absorption at lower temperatures. Thus, it is valuable to determine how clouds of suitable fine particles behave when heated rapidly in hydrogen and other gases.

A cylindrical xenon flash tube with an effective blackbody temperature of approximately $8,000^{\circ}\text{K}$ and a pulse length of about 2 msec is used to simulate the energy spectrum of the fissioning core and the dwell time of the propellant in the core region. The flash tube is placed at one focus of an elliptical reflector; a quartz tube of similar size is held at the other focus. Seeded gases are fed into the quartz tube. The pressure rise during a flash, detected with a fast response pressure transducer, gives an approximate measure of the temperature rise.

Experimental investigations are underway to determine the behavior of, and the maximum temperature attainable with, clouds of graphite, tungsten, iron, tantalum carbide, and tungsten carbide in helium and hydrogen gases.

Further refinement of existing analysis of the transient temperature response of a gas heated by an absorbing cloud, including heat transfer to the cell walls is also planned. However, early results suggest other analytic problems of corresponding importance.

Experimental Apparatus

Flash Tube and Reflector Assembly. - Following generally the design of Hronik et al. (ref. 1), elliptical ribs were machined and joined together with spacers. An Alcoa aluminum "lighting sheet" was cut, formed to the elliptical shape, and attached to the ribs with an epoxy bead. This produced an elliptic cylinder 6.5 in. high, with an 8.0-in. major axis, 7.6-in. minor axis, and 2.5-in. distance between foci. Polished end plates simulate an infinite cylinder length. The entire assembly is made in two halves which can be separated along the major

axis for easy access to the flash tube and absorption cell. The flash tube, an EG&G FX-47B with a 6.5-in. arc length, is mounted in a C-shaped micarta frame. The 2 in. of each arm nearest to the flash tube are micalex to avoid charring during the heat flash. This frame holds the flash tube along one focal line of the ellipse.

The absorption cell, a 6.5 in. length of quartz tubing with a 13-mm inner diameter and a 19-mm outer diameter, is supported along the other focal line by a heavy triangular frame bolted at the vertices to withstand the pressure pulse. The individual parts are bolted to a micarta base to maintain them in the proper relative positions. Photographs of the entire system and of the open reflector are shown in figs. 1 and 2, respectively.

Both ends of the quartz tube are ground flat and smooth and press against O-ring seals. Originally, the O-ring grooves were cut in Circle Seal shutoff valves built into the triangular frames at each end of the absorption cell. A Kistler quartz crystal pressure transducer was mounted on the side of one valve. This transducer read the pressure in the cell through a 1/8-in. diam channel that was 3/8 in. long.

Although this arrangement made it possible to flow gases through the quartz tube and to open or close the valves independently, some difficulties were encountered. To avoid valve leaks during the pressure pulse, the valve core O-rings were sealed on the side opposite the tube. This introduced a dead space or volume of gas not heated by the flash. The combined dead space from both valves and the channel to the transducer amounted to nearly 20% of the heated volume. The rotary O-ring seals developed leaks because of O-ring failure or clogging with powders.

In the revised arrangement, a check valve has been installed at the bottom of the tube with the O-ring groove cut into it. This valve will open with an external pressure of greater than 1 psi above internal pressure to permit gas entry but has positive sealing under internal pressure rise. A needle valve is built into this check valve to aid in purging the tube. The pressure transducer has been mounted at the top of the tube in place of the upper Circle Seal valve. It therefore sees the pressure directly, essentially eliminating all dead space. It was necessary to shield the transducer against the light pulse which registered as a negative pressure as a result of thermal distortion of the transducer housing.

Flash tube energy is supplied by a 1920 μ f capacitor bank charged to 3 kV and triggered by a 25 kV trigger generator. Originally, the tube was operated in series with an 850 μ hy choke in accordance

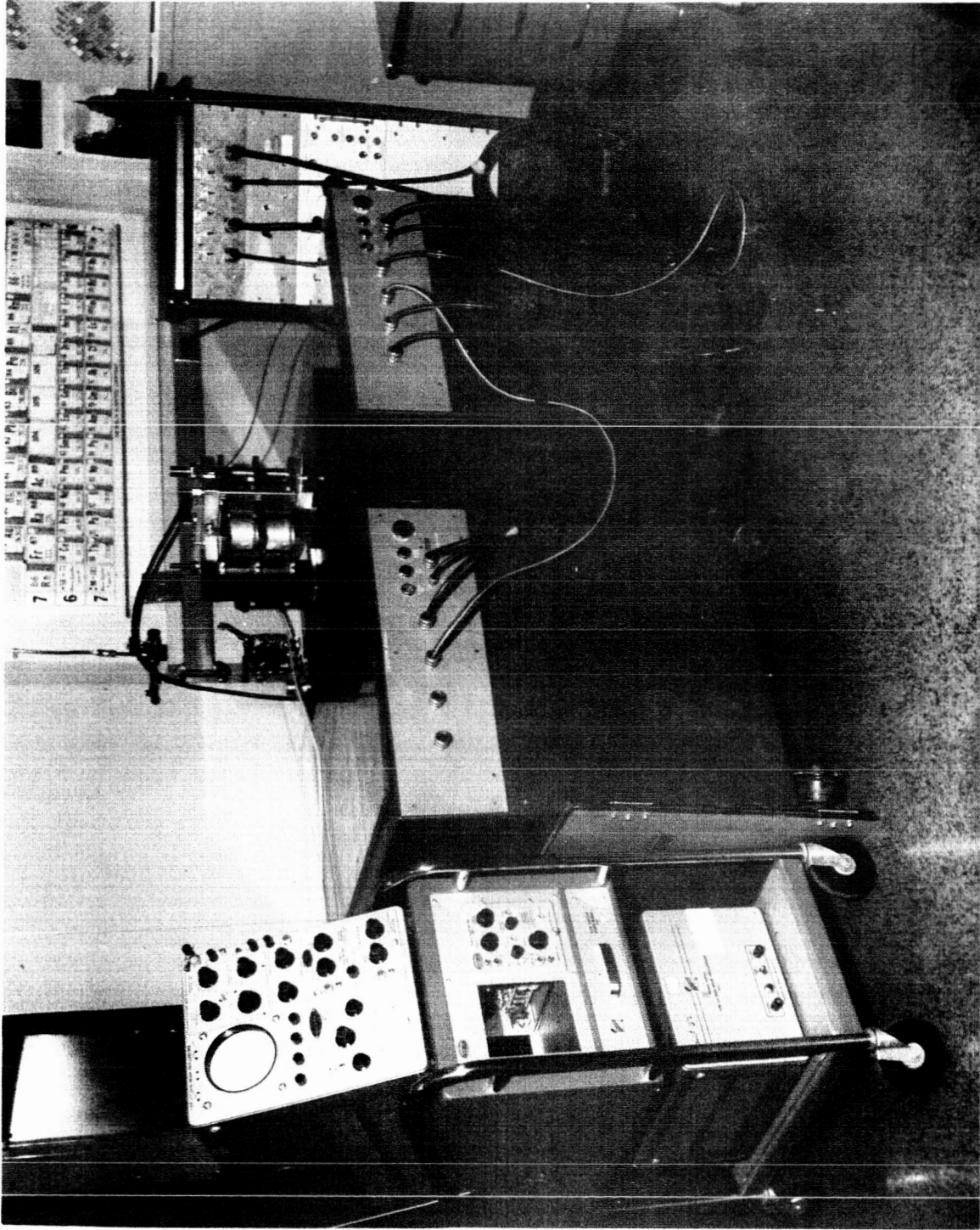


Figure 1. Apparatus for Maximum Temperature Rise Measurements

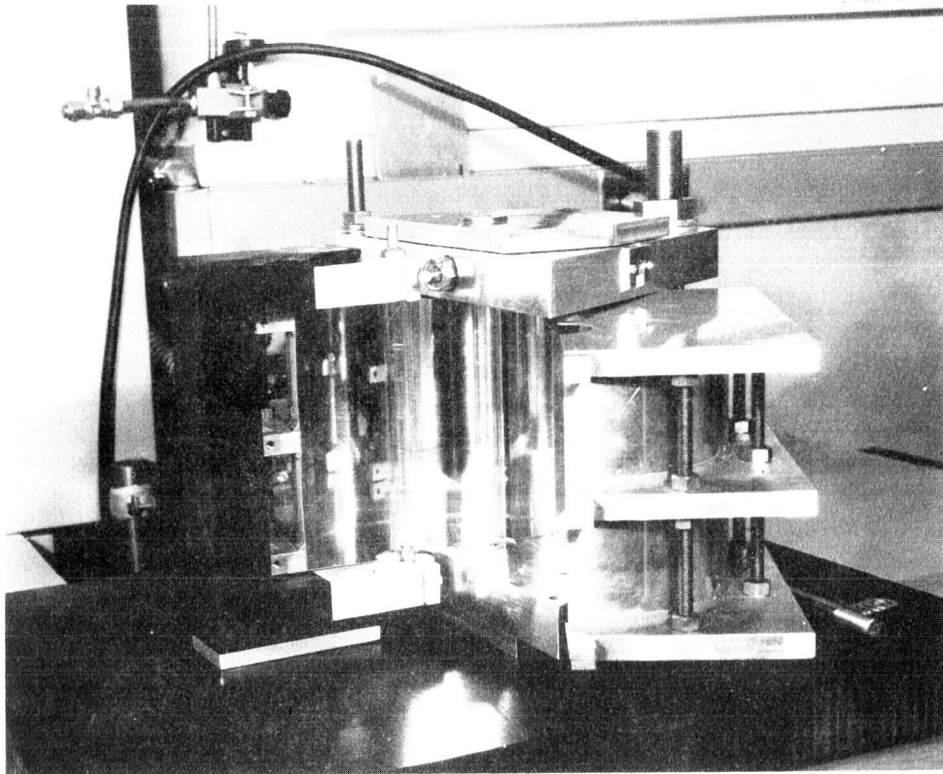


Figure 2. Elliptical Reflector Assembly Open

with the manufacturer's suggested values. An oscillation of the discharge circuit was detected which resulted in a double-peak light pulse. To achieve critical damping without increasing circuit resistance, a new choke was wound and placed parallel to the original coil. This reduced the inductance to $175 \mu\text{hy}$. Circuit resistance external to the flash tube was reduced to a minimum of about 0.2 ohms by using heavy bus bars and taking care with each connection (the resistance of the FX-47B at full power is about 0.5 ohms). The resulting single pulse is about 1.5 msec measured between one-third maximum intensity points, is safely away from the explosive limit of the tube, and gives satisfactorily efficient utilization of the electrical energy.

Dust Feed.— Ideally, a dust feed device would allow the operator to introduce a known density of uniformly sized small particles into a gas. That density would remain constant under fixed conditions but could be varied at will by changing the feed rate.

Devices intended for this purpose are commercially available. One of these, the Wright dust feed mechanism, was purchased and tested. It employs a blade to scrape the packed powder surface as it is advanced at a rate dependent on gear selection. The scraped powder is picked up by the gas stream, dispersed through the high speed region of a jet, and impacted against a plate to break up remaining aggregates. As the feed was found to be non-uniform in time, the cloud was fed into a surge tank from which a more uniform cloud could enter the absorption cell. Because graphite was expected to be most difficult of the powders to disperse, initial work was concentrated on graphite of nominally 1μ diam. A satisfactory cloud was not obtained with the Wright mechanism; the gas emerging from the device contained an appreciable number of particles greater than 20μ in diameter and few of the 1μ -size particles. In addition, the Wright mechanism will not operate under pressure without modification. It was therefore decided to try other methods.

Without the Wright device, the surge tank was found to be unnecessary and to contribute to agglomeration, which occurs very rapidly in graphite suspensions. To allow the graphite to enter the absorption cell as rapidly as possible, a new device was built. This consisted of a threaded cap screwed into the outer side of the entrance valve. A measured amount of powder was dropped into a cavity in the cap. Gas was directed down on the powder from a side tube. When the valve was opened, gas pressure blew the powder into the cell. This system resulted in good graphite dispersion when a Bell flow valve (used in the dairy industry for homogenizing milk) was inserted. This is essentially a compressed mass of fine wire resulting in a large number of narrow channels.

For materials other than graphite, it was necessary to eliminate the homogenizer and to direct the gas up through the powder. This arrangement is shown in fig. 3a. Good dispersion was found under these circumstances. However, the amount of powder actually entering the cell was not known. Some efforts were made to catch and weigh the powder and compare it with optical absorption measured through the tube; but the results were not consistent.

To overcome this problem, the dust feed was further modified by putting the powder cup inside the valve as shown in fig. 3b. A known weight of powder is placed in the cup and all of it is dispersed. This system has the further advantage that the dust does not pass through the entrance valve so that this source of valve leakage is eliminated.

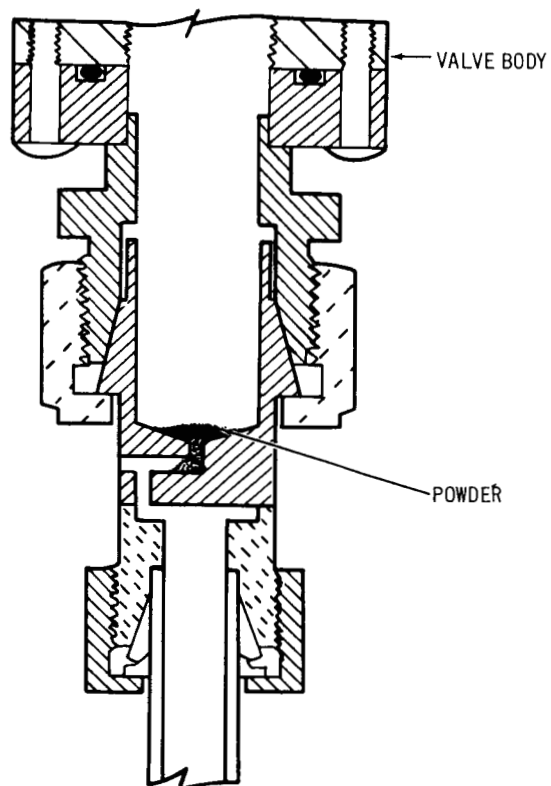


Figure 3a. Powder Outside Valve

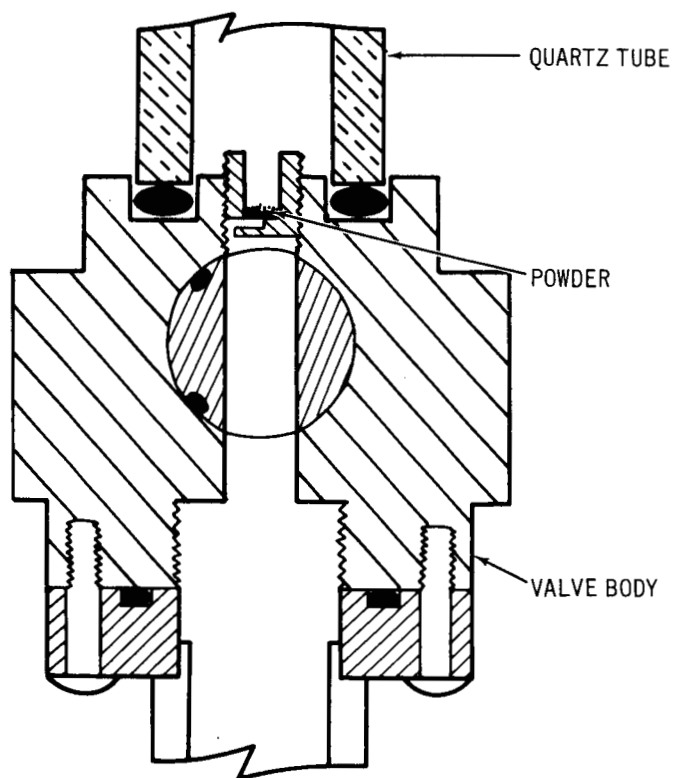


Figure 3b. Powder Inside Cell

The current method uses the powder cup inside the check valve. A solenoid valve is inserted in the gas line outside the check valve. The relay which opens the solenoid valve also activates a variable time delay circuit which, at the end of its delay, triggers the flash tube. It is possible to fire the flash tube from a few milliseconds to 500 msec after the valve is opened. However, nearly 100 msec is required to fill the absorption cell; therefore, delay times shorter than this are not used. Further modifications, particularly in gas flow rate, are being attempted to minimize tube wall coating; but the temperature rise measurements reported here were made using this dust feed.

Experimental Measurements

Graphite Rod Temperature Rise.- The amount of energy available for heating the gas can be estimated from the following considerations. Taking circuit losses into account, the electrical input to the flash tube is about 6,160 J at 3 kV. According to EG&G, the flash tube manufacturer, the optical output is about 50% of the electrical input or about 3,080 joules. Schuldt and Aagard (ref. 2) have calculated the geometrical efficiency of an elliptical reflector of given eccentricity for various relative sizes of source, receiver, and major axis. In this case, the eccentricity is about 0.3, the source size is 1/2 in., and the semi-major axis is 4 in. For a 1/2-in. receiver, their value of geometrical efficiency is about 0.75. The average reflection coefficient of the aluminum over the wavelength range is also about 0.75 so that about 1,730 J should impinge on a 1/2-in. diam volume at the focus. Of this total, 10% will be reflected by the quartz tube. Therefore, 1,560 J or 370 cal should then be available inside the absorption cell. Kuebler and Nelson (ref. 3) used graphite spectroscopic electrodes to compare the focused energy of a group of flash tubes. They determined the surface reflection of the graphite to be about 0.25. The rest of the incident energy was absorbed by the graphite and the resultant temperature rise was measured by a thermocouple.

In this experiment, a 1/2-in. diam graphite spectroscopic electrode was instrumented with a 28-gage chromel-alumel thermocouple containing a 1/16-in. hole drilled to the center. The thermocouple output was observed on an oscilloscope and on a recorder with good agreement. Maximum temperature was attained in a few seconds followed by slow cooling. For a 3 kV flash, the maximum temperature for the graphite rod inside a quartz tube was measured as 53°C. The graphite has a mass

of 32.32 g and a specific heat of 0.17 so that 290 cal were absorbed. If 25% were reflected by the graphite surface, 390 cal were incident on the volume. This compares reasonably well with the value estimated above.

Particle Density.- While the graphite rod reflects or absorbs all the incident energy, the seeded gas transmits a fraction of the incident light depending on the material and the seed density. For 1.4μ diam carbon particles, Lanzo and Ragsdale (ref. 4) found the transmitted fraction of the incident light through 10 cm of a suspension of 1×10^{-4} g/cc, to be $I/I_0 = 0.02$. For a 1-cm path length, this would lead to about 68% transmission; that is, absorption of roughly 30% of the light incident on the absorption cell. A reasonable graphite seed for this experiment is therefore about 2×10^4 g/cc of micron-size particles in suspension.

With the present dust feed method, the desired amount of powder is weighed out and placed in the cup. For graphite, this may be 1 to 4 mg; for other materials, it is 10 to 20 mg. In each case, the entire amount is dispersed in the 22 cc volume of the absorption cell. The major uncertainty lies in what fraction of this is in suspension and what fraction is adhering to the walls.

Particle Size Distribution.- To estimate the size distribution of the particles in the cloud and to roughly determine the amount of agglomeration, millipore filters were introduced and allowed to capture the particles. A filter holder with a backing screen was interposed between the seeding device and a closed container simulating the absorption cell.

However, a cloud of the density necessary for absorption coated the filter so heavily it was not possible to examine individual particles. Using a much thinner cloud than that required for absorption, samples were caught on millipore filters and examined. There are two difficulties with this procedure. A denser cloud may experience more agglomeration than was indicated so that this method underestimates the average particle size. On the other hand, some agglomerates may have occurred on the filter, not in suspension, so that this method overestimates the average size. It is not known how much one of these effects compensates for the other, so the results can only be regarded as an indication of the particle size distribution. Fig. 4 is a typical electron micrograph of the TaC powder. The TaC particles appear black against a gray filter. While some 10μ and other large particles are evident, there are a large number of particles down to about 0.1μ .

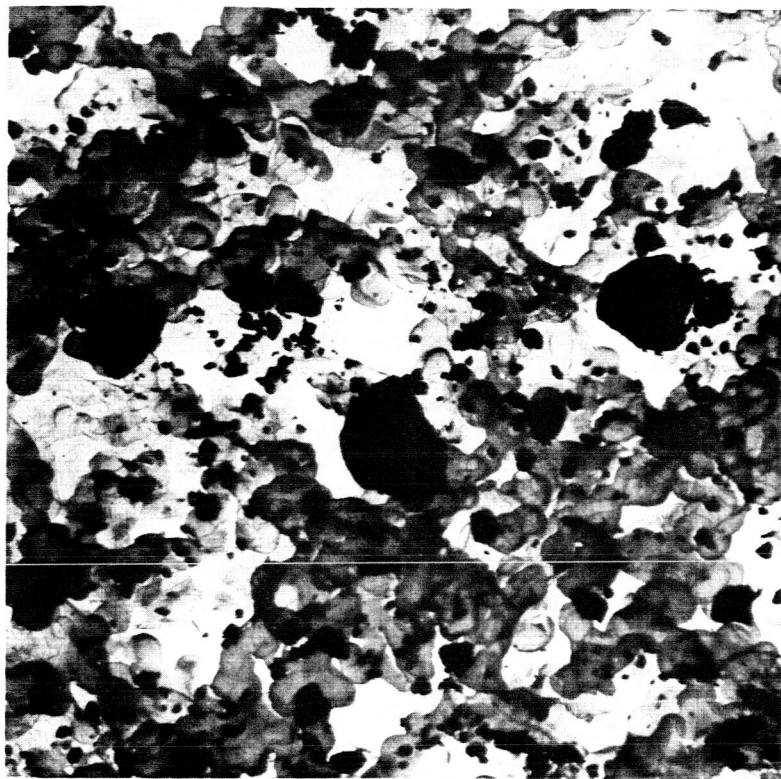


Figure 4. Electron Micrograph of TaC Dispersion Caught on Millipore Filter (1/4 in. $\approx 1\mu$)

Absorption of Seeded Gas.- In spite of the complexities of particle dispersion, it was possible to determine the absorption of the cloud in a straightforward manner. This was done using pairs of small holes cut in the reflecting ellipse on opposite sides of the absorption cell. One pair of holes was about 1-3/4 in. from the top of the cell; the other pair was about the same distance from the bottom. A small dc lamp with lens was positioned outside one upper and one lower hole and an SD-100 photodiode was placed at each opposite hole to receive the transmitted beam. It was necessary to use black paper with suitable holes cut in it to line the elliptical reflector and to avoid internal reflections. With this precaution, the two detectors were each sensitive only to variations in the corresponding light source and showed no interdependence. The diode output was terminated in a 1,000-ohm resistor in each case and the signal fed to an oscilloscope. The photodiodes have linear response over a wide range of intensity. Light transmission measurements were made before and during admission of the seed cloud.

By following the pressure rise with the pressure transducer as gas was admitted to the system, it was found that from the opening of the solenoid valve, about 90 msec was required to fill the absorption cell. The time delay circuit is adjustable from a few to about 500 msec; the absorption measurements were recorded to 500 msec.

The transmission measurement in the lower half of the cell indicated that the powder was deposited on the walls within 50 msec of valve opening and the transmission remained almost constant thereafter. The value measured several minutes later differed only slightly from the 0 to 500 msec value (Table I). In the upper half of the tube, oscillations in the transmitted light demonstrated swirling of the suspension. The amount of absorption was typical of each cloud and showed an average value that remained constant over 500 msec. But several minutes later the transmission in each case can be seen from Table I to be increased because of cloud settling.

TABLE I
OPTICAL TRANSMISSION THROUGH ABSORPTION CELL

Seed	Gas	% Transmission			
		Upper Half		Lower Half	
		0-500 msec	3 min	0-500 msec	3 min
10 mg TaC	10 atm He	45		55	
10 mg TaC	5 atm He	25	55	55	50
10 mg backed TaC	5 atm He	40	65	70	60
20 mg TaC	10 atm He	10		40	
20 mg TaC	5 atm He	15		35	
10 mg Fe	5 atm He	40		30	
20 mg Fe	10 atm He	20		40	
20 mg Fe	5 atm He	15		20	
10 mg WC	10 atm He	60	75	50	50
10 mg WC	5 atm He	60		55	
20 mg WC	10 atm He	50		35	40
20 mg WC	5 atm He	40	65	30	30
20 mg W	10 atm He	80	85	95	100
20 mg W	5 atm He	90		95	
1 mg C	10 atm He	65	85	75	80
	5 atm He	65	85	70	65
2 mg C	5 atm He	45		65	

It is concluded from these results that a flash occurring any time in the interval from 100 to 500 msec after the opening of the valve should result in the same amount of energy absorption. The measured transmission values are listed according to seed material in Table I. Fig. 5 shows typical curves for absorption in the upper and lower halves of the absorption cell.

To compare these data with those of Lanzo and Ragsdale, the measured transmission values in the upper half of the absorption cell are converted to coefficient per particle versus particle radius and compared with fig. 10 of ref. 4.

From

$$\frac{I}{I_0} = e^{-\alpha X} \quad (1)$$

with X = absorption cell diameter, α is found from the transmission measurements listed in Table I. The particle concentration, N , is calculated from

$$N = \frac{1}{\frac{4}{3} \pi r^3} \frac{\rho_p}{\rho_s} \quad (2)$$

where

$$\begin{aligned} r &= \text{particle radius} \\ \rho_p &= \text{particle density in g/cm}^3 \\ \rho_s &= \text{material density in g/cm}^3 \end{aligned}$$

Because there is a considerable particle size range in most of the materials, an average value must be used. Table II shows the values used for r and the calculated N values. A uniform cloud is assumed with the total mass of powder dispersed in the 22 cc of the absorption cell. Thus the reduction in N caused by wall deposition is neglected in this comparison.

In fig. 6, the value for α/N versus r are plotted on a portion of Lanzo and Ragsdale's curve which has been extended to $\alpha/N = 10^{-5}$. The agreement is reasonable and within the uncertainties of the measurements.

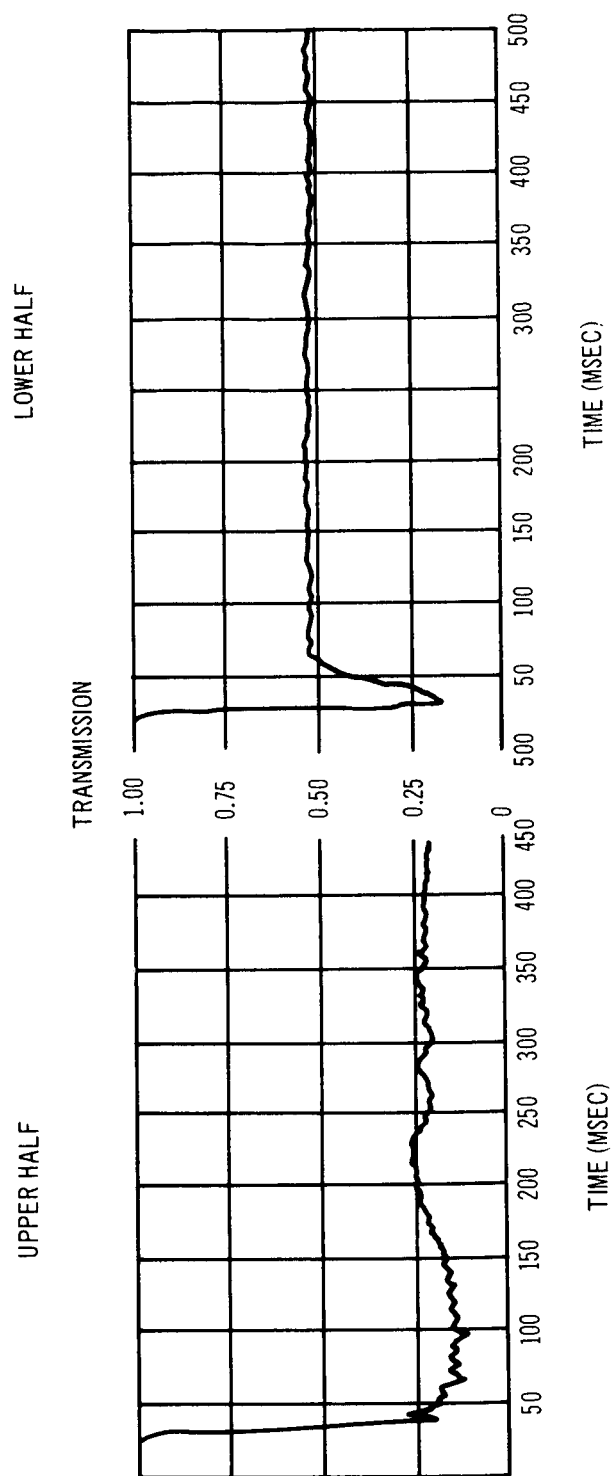


Figure 5. Oscilloscope Trace of Light Transmitted Through Upper and Lower Halves of Absorption Cell
After Injection of 10 mg TaC in 5 atm of Helium

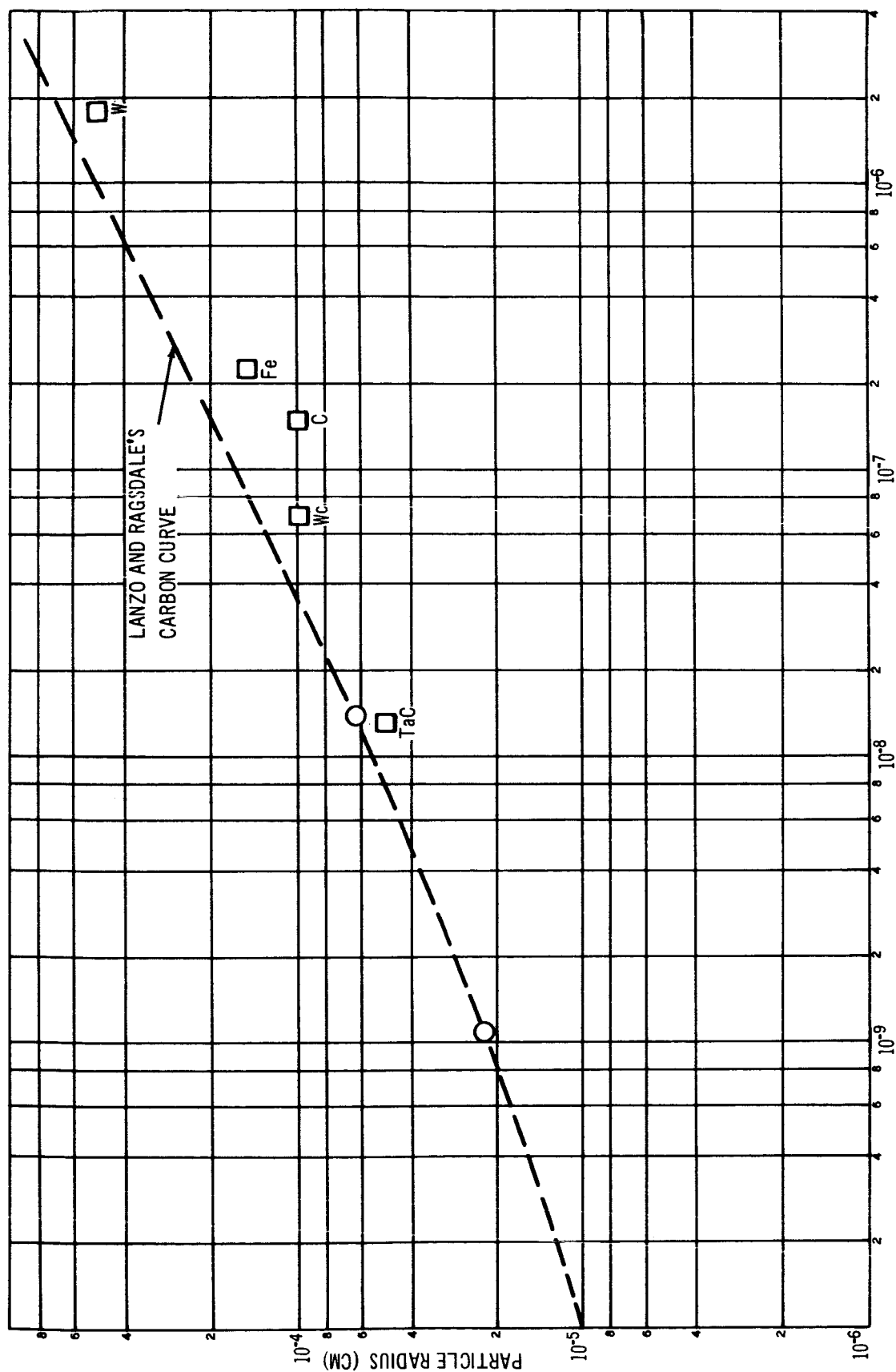


Figure 6. Correlation of Absorption Data

TABLE II
SEED PARTICLE CONCENTRATIONS

Material	r (cm)	g/cm ³	N cm ⁻³
TaC	5.0×10^{-5}	14.6	6.3×10^7
WC	1.0×10^{-4}	15.7	7.0×10^6
Fe	1.5×10^{-4}	7.8	4.1×10^6
W	5.0×10^{-4}	19.3	9.1×10^4
C	1.0×10^{-4}	1.6	6.4×10^6

Temperature Rise Measurements. - To make a temperature measurement, gas flows into the cell to disperse the powder. The flash tube is triggered after the selected time delay. The pressure seen by the transducer is displayed on an oscilloscope together with the light pulse as seen by a photodiode. Fig. 7 shows a typical view of the two pulses. The oscillation on the pressure pulse may be due to shock waves caused by nonuniform heating along the length of the cell. The starting pressure is known; the peak pressure is determined from the pulse height and transducer calibration. The temperature rise is taken as proportional to the pressure rise.

Maximum temperature rise has been measured in helium for TaC, WC, Fe, W, and graphite. Most of the measurements were made with 5 atm of gas and with suitable weights of powder to give reasonable absorption. In Table III, the percentage of absorption is that measured in the upper half of the cell with the photodiode. The energy absorbed is calculated from the percent absorbed by the cloud and the available energy from the graphite cylinder calorimeter results. The calculated potential temperature rise values are calculated assuming no radiation losses and no change of absorption with temperature for some typical clouds. The measured temperature rises shown in the last column are not as high as were expected from the energy absorbed.

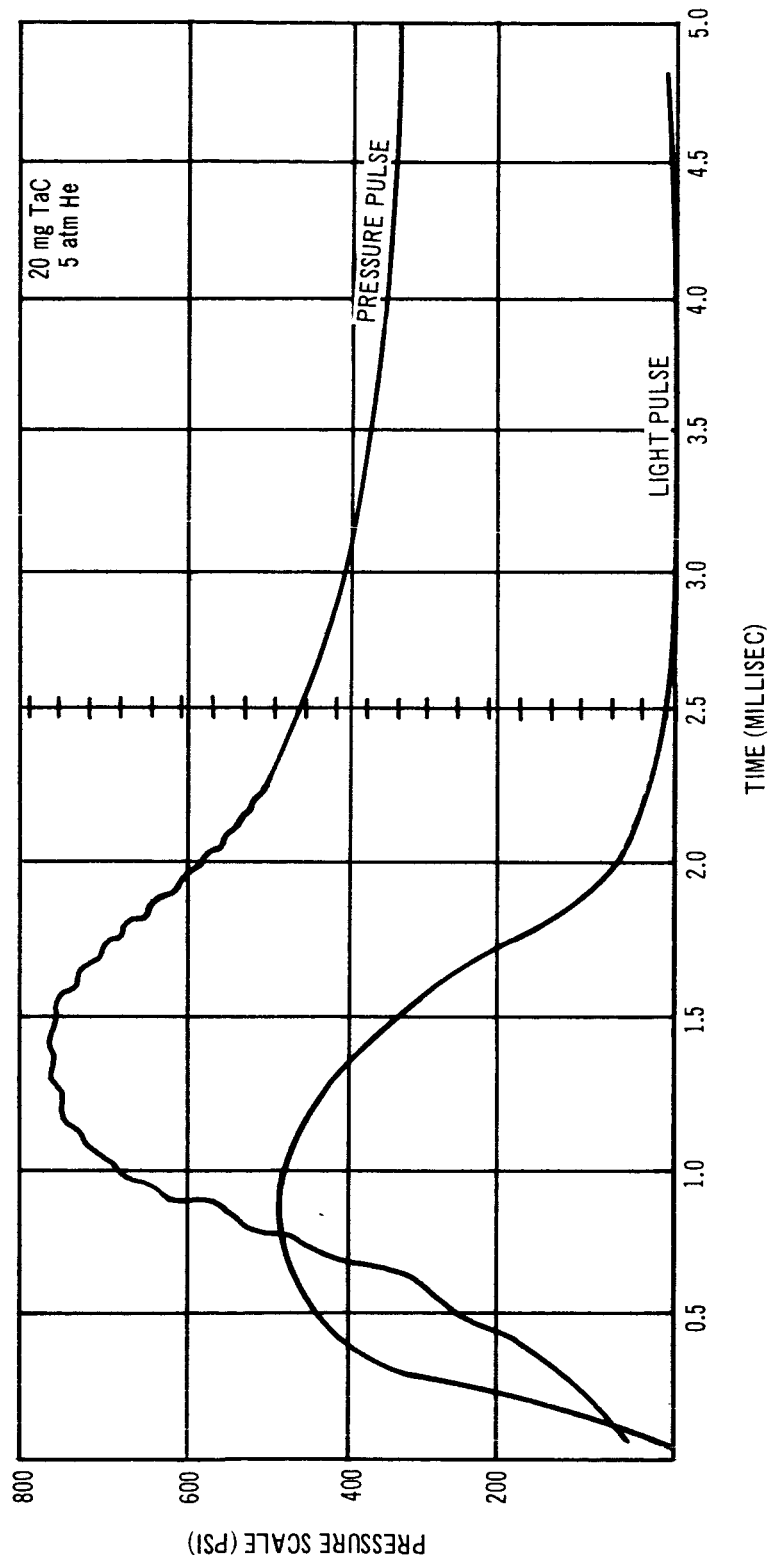


Figure 7. Oscilloscope Trace of Typical Light and Pressure Pulse

TABLE III
CALCULATED AND MEASURED TEMPERATURE RISES

Seed	Seed Heat Capacity (cal/°C)	Heat Capacity (5 atm He)	Measured Absorption (%)	Calculated Energy Absorbed (Cal)	Calculated Temperature Rise (No Losses) (°C)	Measured Max. Temp. (°C)
10 mg TaC	$<0.1 \times 10^{-2}$	1.3×10^{-2}	55	215	15,000	3,000
10 mg WC	$<0.1 \times 10^{-2}$	1.3×10^{-2}	40	156	11,000	1,600
10 mg Fe	$\sim 0.16 \times 10^{-2}$	1.3×10^{-2}	60	234	16,000	3,000
20 mg W	0.08×10^{-2}	1.3×10^{-2}	10	39	2,800	1,000
1 mg C	0.05×10^{-2}	1.3×10^{-2}	35	137	10,000	2,500

DISCUSSION

Temperature Rise Limitation

Radiation will provide a limitation at some temperature below that of the flash tube. It is of interest to determine whether this causes the observed upper limit of $3,000^{\circ}\text{C}$. Assuming the particle sizes listed in Table II, the total surface area of all the particles was found. An upper limit on radiation loss was determined by using the entire surface area of the powder and assuming an emissivity of 1. Even at $5,000^{\circ}\text{K}$, the energy radiated in 2 msec is less than 30% of that absorbed.

It is clear that radiation losses cannot be responsible for limiting the temperature rise at $3,000^{\circ}\text{C}$. The explanation is more likely to lie in the change in absorption with temperature.

In the case of Fe, the boiling point at $3,000^{\circ}\text{C}$ is a reasonable upper limit, although the vapor may also effect some absorption, thus allowing a further increase. The iron vapor itself would contribute only about 2 psi to the pressure, so this influence would not be clearly detectable.

With the other materials, particle evaporation should not be significant at temperatures up to $3,000^{\circ}\text{C}$. Dissociation of the carbides could be a factor in the temperature limit; chemical reaction with adsorbed gases seems to be a probable cause. In the case of TaC, some efforts have been made to outgas the powder by heating in vacuum; but, in spite of this method, a white Ta_2O_5 residue has been found after each flash. Graphite reaction with the quartz tube wall has been discussed in earlier monthly reports. Where graphite has been in contact with quartz, it has reduced the wall material leaving a brownish Si coating. If adsorbed oxygen is also present, oxidation of particles not in contact with the wall should also occur. In either case, formation of transparent CO and/or CO_2 could limit the temperature rise.

Chemical analysis of residual powders is being undertaken whenever adequate quantities can be collected. Efforts will also be made to analyze the residual gases, although the results are not expected to be as exact.

In addition, a spectrograph will be set up to examine emission and absorption spectra to gain an understanding of the processes occurring during the temperature rise.

Another mechanism which may limit the average temperature rise is the distribution of absorbing particles. The deposition of particles on the wall of the absorption cell has already been observed and is an extreme example of this process. In this case, particles deposited on the wall limit the energy entering the active volume of the adsorption cell and limit the number of absorbing centers in the active volume. Removal of this extreme limit is expected as the particle dispersion mechanism is improved. However, similar processes may take place entirely within the gas phase of the absorption cell. Thus, high absorption near the wall will insulate the interior of the adsorption cell in much the same way as anticipated in gaseous core reactor concepts. Systematic variation of seed density will help to clarify this possibility.

Analytical Work

The physical system of interest consists of a dispersion of solid particles in a gas which is essentially transparent to thermal radiation. Radiant energy is absorbed by the solid particles. This absorbed energy then is conducted inward to heat the solid absorber and outward to heat the gas. To treat the results of the present flash heating experiment as well as gaseous core reactor applications, a general description of this system should be established.

Consider first a system of uniformly distributed, solid, spherical particles of radius r and of number density n particles per cubic centimeter. For a uniform particle distribution, each particle can be assumed to be located at the center of a cubic unit cell of side d . The number density n is then

$$n = \frac{1}{d^3} \quad (3)$$

The absorption of radiant energy is expressed by

$$I = I_0 e^{-\alpha X} \quad (4)$$

where $\alpha = n\sigma$ and σ is the absorption cross-section for each particle. It is convenient to express the absorption cross-section as a constant a times the geometric cross-section or

$$\sigma = a\pi r^2 \quad (5)$$

The absorption coefficient α is then

$$\begin{aligned} \alpha &= n\sigma \\ &= \frac{a\pi r^2}{d^3} \end{aligned} \quad (6)$$

Within this framework, it is desirable to find general expressions for the particle to gas mass ratio and the corresponding heat capacity of the gas and particle suspension.

The mass of particles per unit volume is defined as ρ_p and the particle material density ρ_s . The expression for ρ_p is then

$$\begin{aligned} \rho_p &= n \times \frac{4}{3}\pi r^3 \rho_s \\ &= \frac{4\pi}{3} \left(\frac{r}{d}\right)^3 \rho_s \end{aligned} \quad (7)$$

The gas density, ρ_g , written in terms of density at STP, ρ_o , and dimensionless pressure P^* and temperature T^* is then

$$\rho_g = \rho_o \frac{P^*}{T^*} \quad (8)$$

The ratio of solid particle to gas density is then

$$\begin{aligned} \frac{\rho_p}{\rho_g} &= \frac{\frac{4}{3}\pi \left(\frac{r}{d}\right)^3 \rho_s}{\frac{P^*}{T^*} \rho_o} \\ &= \frac{4\pi r^3}{3a} \times \frac{T^*}{P^*} \times \frac{\rho_s}{\rho_o} \end{aligned} \quad (9)$$

The corresponding heat capacity ratio is

$$\frac{\rho_p C_{vp}}{\rho_p C_{vg}} = \frac{4r\alpha T^*}{3aP^*} \times \frac{\rho_s C_{vs}}{\rho_o C_{vg}} \quad (10)$$

For the gases and solids of particular interest in this work, representative values of ρ , C_v and ρC_v are collected in Table IV. Gas values refer to STP while the data on solids reflects specific heat values at 1,000°C.

TABLE IV
HEAT CAPACITY VALUES

		ρ_{gm}/cm^3	$C_v \text{ cal/gm}^\circ C$	$\rho C_v \text{ cal/cm}^3 \circ C$
Gases	He	0.178×10^{-3}	0.753	1.34×10^{-4}
	A	1.78×10^{-3}	0.0752	1.34×10^{-4}
	H ₂	8.98×10^{-5}	2.40	2.16×10^{-4}
Solids	C	2.2	0.45	0.99
	Ta	16.6	0.043	0.71
	W	18.6	0.036	0.67
	TaC	14.6	0.062	0.92
	Fe	7.8	0.16	1.25

From this simple representation, several general conclusions result. First, the solid to gas density ratio is proportional to $\frac{r\alpha}{a}$ for given materials. Second, the heat capacity ratio is proportional to the same quantity with little dependence on the gas or solid materials involved. These relationships are important in displaying the effect of alternate gases, solid particles, and particle sizes.

The next area of interest is the transient response of such a system of solid particles dispersed in a gas. Several analyses have demonstrated the very rapid response of the system in which solid particle temperature gradients are negligible and in which the maximum temperature difference between the solid and the gas is asymptotically

$$T_p - T_o = \frac{\beta}{24K} \times \frac{d^3}{r} \quad (11)$$

where β is the rate of temperature rise in the gas and K the thermal diffusivity of the gas. Expressed in terms of α and a , this relation becomes

$$T_p - T_o = \frac{\beta}{24K} \times \frac{a\pi r}{\alpha} \quad (12)$$

Loss of heat by conduction and reradiation during the flash duration has previously been predicted to be small. This analysis is largely confirmed by comparison with measured cooling rates following a flash. For values of β observed during the flash, maximum particle gas temperature differences of about 100°K are typical.

Further analytical refinement was originally expected to treat more accurately the transport properties of dissociating hydrogen as they reflect the transient behavior of a flash heated absorption cell. However, current experimental results suggest that a more detailed treatment of absorption in a polydisperse particle system may be equally or more significant. Relative emphasis on these two refinements will be guided by future measurements.

Future Work

The next effort will be to measure maximum temperature rise in hydrogen. In addition, efforts to improve the cloud injection and to minimize wall coating will continue along with a systematic study of temperature rise versus absorber concentration. Following those measurements, the work of greatest immediate interest is that of emission and absorption spectroscopy. A Jarrell-Ash high-speed 0.5-m spectrograph will be set up to focus on the absorption cell. If there is sufficient emitted light, an effort will be made to identify the chemical species present from their emission spectra. However, it may be that, at these temperatures, the amount of emission will not be sufficient to make identifications. It is also planned to use a second flash tube of shorter duration and less intensity, the FX-33. This, used with a time delay, will be flashed at chosen times after the FX-47B so that the absorption spectra can be studied during and after the heating pulse. The course of future analysis will be guided by the development of experimental effort.

The major problem ahead seems to be to resolve the differences between absorption measured at low temperature and the much lower absorption inferred from the pressure rise observed in the absorption cell. Future experimental and analytic effort will be directed toward resolution of this difference.

PRECEDING PAGE BLANK NOT FILMED.

REFERENCES

1. Hronik, Richard H.; Jones, Roger C.; and Bronco, Charles J.: Rev. Sci. Instr. vol. 33, p. 776, 1962.
2. Schuldt, S. B.; and Aagard, R. L: Applied Optics vol. 2, p. 509, 1963.
3. Kuebler, N. A.; and Nelson, L. S.: Jour. Opt. Soc. Am. vol. 51, p. 1411, 1961.
4. Lanzo, Chester D.; and Ragsdale, Robert G.: NASA TN D-1405, Sept. 1962.